PAPER *Joint Special Section on Opto-electronics and Communications for Future Optical Network*

Impact of Sampling and Quantization on Kramers-Kronig Relation-Based Direct Detection

Takaha FUJITA[†a)], **Kentaro TOBA**[†], ***Nonmembers***, **Kariyawasam Indipalage Amila SAMPATH**[†], ***and*** **Joji MAEDA**[†], ***Members***

SUMMARY Impact of sampling frequency and the number of quantization bit of analog-to-digital conversion (ADC) in a direct detection lightwave system using Kramers-Kronig (KK) relation, which has been attracting attention in recent years, are numerically investigated. We studied the effect of spectral broadening caused by nonlinear operations (logarithm, square root) of the KK algorithm when the frequency gap (shift frequency) between the modulated signal and the optical tone is varied. We found that reception performances depend on both the ADC bandwidth and the relative positions of the optical tone and the spectrum. Spectral broadening caused by the logarithm operation of the KK algorithm is found to be the dominant factor of signal distortion in an ADC bandwidth limited system. We studied the effect of the number of quantization bit on the error vector magnitude (EVM) of KK relation based reception in a carrier-to-signal power ratio (CSPR) adjustable transmission system. We found that performances of KK relation based receiver can be improved by increasing the number of quantization bits. For minimum-phase-condition satisfied KK receiver, the required number of quantization bit was found to be 5 bits or more for detection of QPSK, 16-QAM and 64-QAM-modulated signal after 20-km transmission.

key words: *Kramers-Kronig relation, direct detection, digital signal processing, analog-to-digital conversion, signal-signal beat interference*

1. Introduction

With the recent increase in mobile traffic, there is an increasing demand for low-cost, large-capacity lightwave systems for intra- and inter-data center optical links [1]. The digital coherent detection can increase the capacity by optimizing the spectral efficiency, however, it is not desirable from the viewpoint of cost, particularly in short-reach links [2]. The complex configuration of the receiver increases both the cost and the power budgets. Single-polarization intensity-modulated direct-detection (IM-DD), where the detection is performed using a single photo-detector (PD), is a low-cost solution preferable for short-reach links. However, since the degree of freedom for modulation is limited only to the optical intensity in single photo-detector based IM-DD systems, the transmission capacity of the system is limited by the receiver noise and the system-induced waveform distortions [3]. Moreover, fiber dispersion limits the transmission distance in IM-DD systems due to the inability of using electronic dispersion compensation (EDC) at the receiver [4].

Manuscript received December 20, 2019.
Manuscript revised April 3, 2020.
Manuscript publicized June 8, 2020.

[†]The authors are with Department of Electrical Engineering, Graduate School of Science and Technology, Tokyo University of Science, Noda-shi, 278-8510 Japan.
a) E-mail: takaha.fujita@gmail.com

DOI: 10.1587/transcom.2019OBP0008

Optical single sideband (SSB) modulation was being studied to circumvent the issue of fiber dispersion. SSB modulation tolerates the fiber dispersion because of the reduced bandwidth compared to the double-sideband (DSB) signal. Moreover, EDC can be performed at the receiver for optical SSB signal because the phase information perseveres even after direct detection [5]. Because of these reasons SSB transmission of pulse amplitude modulation (PAM) signal has been studied as a low-cost solution for IM-DD preferred systems. However, the restricted degree of freedom limits the transmission capacity in such systems [6].

As a way to increase the capacity, optical SSB transmission of optical orthogonal frequency division multiplexing (OOFDM) [7], [8] and Nyquist-pulse shaped subcarrier modulation (Nyquist-SCM) [9] was proposed and studied. OOFDM or Nyquist-SCM signal transmitted along with the optical carrier was direct-detected using a single PD. Nevertheless, signal-signal beat interference (SSBI) generated at the square-law detection degrades the received signal in those systems. A frequency gap has to be maintained between the optical carrier and the signal spectrum to avoid the effect of SSBI which leads to a drop in spectral efficiency.

Several methods have been proposed and studied extensively to mitigate SSBI of direct-detected SSB transmissions [10]–[14]. Among those, the optical field recovery method using Kramers-Kronig (KK) relation shows superior performances [15], [16].

In KK receiver-based transmission systems, the optical field modulated by a complex-valued baseband signal is transmitted along with an optical tone at one edge of the signal spectrum. Since the signal spectrum distributes only in one side respective to the optical tone, the transmitted signal behaves as an SSB signal. At the receiver, direct detection is performed using the transmitted optical tone. Using receiver-side digital signal processing (DSP), the phase of the transmitted signal is calculated directly from the received intensity information after direct detection.

Because the phase of the transmitted signal is calculated using the detected intensity which includes SSBI, no SSBI cancellation is required in KK reception. This eliminates the requirement of the frequency gap between the optical tone and the modulated signal spectrum consequently increasing spectral efficiency. This SSB modulation - self-coherent heterodyne detection (SSB-SCHD) scheme attracts a great interest because of the full field recovery capability after direct detection and consequent signal compensation

capability using DSP.

However, those advantages of the KK receiver come at the expense of strict DSP requirements. KK algorithm consists of three main DSP calculation blocks, namely square-root (sqrt), logarithm (log) and Hilbert transform. Among those, sqrt and log operations are non-linear operations that result in bandwidth expansions. Z. Li et al. [17] reported that x4 or higher oversampling is required to overcome the penalty caused by bandwidth expansion. Approximating sqrt using the second-order binomial expansion and log using the second-order Taylor expansion, T. Bo et al. [18] reported optimized KK reception using x2 oversampling. A. J. Lowery et al. [19] proposed clipping of the detected waveform before the log operation for the digital-to-analog converter (DAC) resolution limited scenarios. In [20] C. Füllner et al. proposed DSP complexity reduction using FIR filter based Hilbert transform.

In DSP related issues, another fact of interest is how the performances of analog-to-digital (AD) conversion affects the performance of KK reception, which is not revealed yet. Because of the nonlinear operations in the KK algorithm, it is considered that high AD conversion accuracy is required, and errors in AD conversion may raise the CSPR requirement to satisfy the minimum phase condition.

In this study, extending the results reported in [21], we numerically examined these concerns, namely, the effect of sampling frequency and the number of quantization bit on the performance of the KK algorithm based direct detection in a 20-km transmission link.

The rest of this paper is organized as follows: In Sect. 2, the reception of the direct-detected signal using KK relation is explained. Details about our simulation model are presented in Sect. 3. The effect of AD quantization is discussed in Sect. 4 following a discussion about sampling frequency and aliasing noise. Conclusions are drawn in Sect. 5.

2. Kramers-Kronig Relation

The KK relation can recover the phase information from the intensity of the received signal after direct detection. The phase recovery block diagram using the KK relation is shown in Fig. 1. In order to apply the KK algorithm, an optical tone with sufficient power must exist at the edge of the modulated signal spectrum (Fig. 2), which is called the minimum phase condition [22]. The minimum phase condition also can be expressed as a relation of the carrier-to-sideband power ratio (CSPR) and the peak-to-average power ratio (PAPR) where CSPR needs to be greater than PAPR [23]. CSPR and PAPR are given in (1) and (2) respectively, where $S(t)$ denotes the modulated signal and A is the optical tone.

$$\mathrm{CSPR} = \frac{|A|^2}{\langle |S(t)|^2 \rangle} \tag{1}$$

$$\mathrm{PAPR} = \frac{\max(|S(t)|^2)}{\langle |S(t)|^2 \rangle} \tag{2}$$

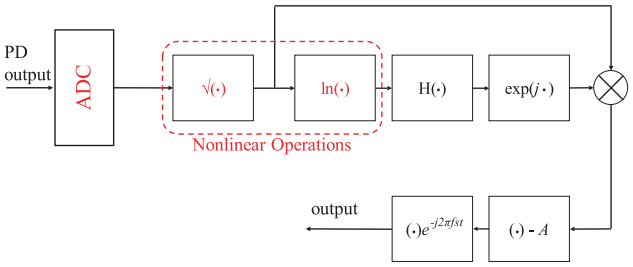

Fig. 1 Block diagram of signal recovery using KK relation.

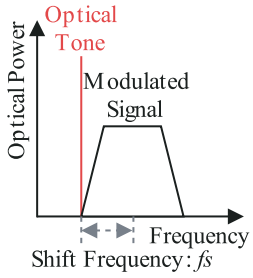

Fig. 2 Spectrum of the minimum phase condition.

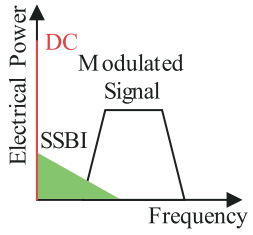

Fig. 3 Spectrum after DD.

To detect using the KK relation, the transmission signal should be single sideband. By inserting the tone to one edge of the modulated signal, the transmission signal is generated as given in (3) where $E(t)$ denotes the transmission signal and f_s is the relative frequency of the modulated signal in regard to the tone. Hereafter, we refer to f_s as the shift frequency.

$$E(t) = A + S(t)e^{j2\pi f_s t} \tag{3}$$

The intensity of the $E(t)$ detected by a single PD can be written as

$$\begin{aligned} |E(t)|^2 &= |A|^2 + A^* \cdot S(t)e^{j2\pi f_s t} \\ &\quad + A \cdot S(t)^* e^{-j2\pi f_s t} + |S(t)|^2. \end{aligned} \tag{4}$$

On the right side of the (4), the original signal information is included in the second and the third terms, and the fourth term is SSBI (see Fig. 3). By applying the KK relation to the signal after direct detection, the phase φ is recovered as in the following equation,

$$\varphi(t) = 0.5 \cdot \mathbf{H}(\ln(|E(t)|^2) \tag{5}$$

where $\mathbf{H}$ denotes the Hilbert transform. By using the calculated phase, the original signal $S(t)$ is recovered as in (6).

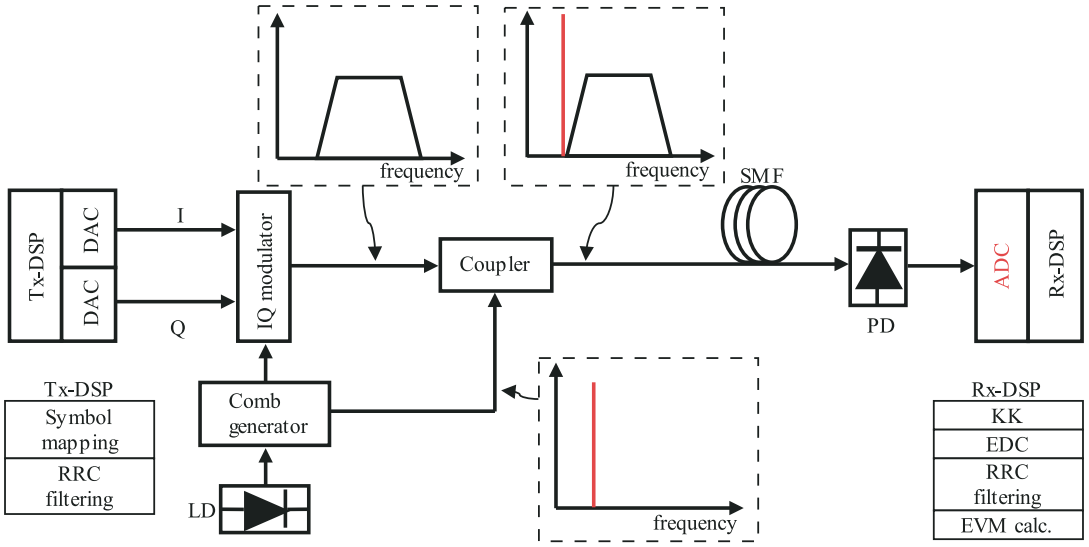

Fig. 4 System under consideration.

Here, I is the photocurrent after direct detection.

$$S(t) = \left\{ \sqrt{I} \exp(j\varphi(t)) - A \right\} e^{-j2\pi f_s t} \tag{6}$$

3. Simulation Outline

We numerically study how the performance of AD converter (ADC) affects the full-field recovery process using the KK relation. Figure 4 shows the system configuration assumed in this study. At the transmitter, after symbol mapping, root raised cosine (RRC) filtering is performed before ideal digital-to-analog (DA) conversion. Light from a comb generator is modulated at IQ modulator by the DACs outputs. Two Mach-Zehnder interferometers (MZIs) of the IQ modulator are biased at their transmission null points. Assuming ideal phase synchronization and polarization matching with the modulated light, a frequency-downshifted optical tone by f_s is added to the modulated signal. This optical tone acts as the local oscillator at the heterodyne detection. The powers of the optical tone and the modulated signal are related to CSPR as given in (1).

At the receiver, the transmitted signal is directly detected by a single PD, sampled and quantized by an analog-to-digital converter (ADC), and digitized. The digitized signal is processed through the KK algorithm and the baseband signal is recovered. Symbols are extracted after electronic dispersion compensation (EDC) and RRC filtering. The received signal is evaluated by measuring the error vector magnitude (EVM).

In this study, we numerically investigated how the relative position of the optical tone and the modulated signal spectrum affects KK reception in an ADC bandwidth-limited system. We also studied the effect of the number of quantization bit of ADC on KK reception. We assumed ideal quantization when investigating the effects of ADC bandwidth limitations, and 128 Sa/symbol sampling when investigating the effects of the number of quantization bit. As our primary intention is to understand the limits of the KK algorithm in terms of ADC sampling frequency (ADC bandwidth) and the number of quantization bit, we ignore all electrical and optical noises on the signal. Table 1 shows the simulation parameters used in our study.

Table 1 Simulation parameters.

Parameter	Value
Modulation format	QPSK, 16QAM, 64QAM
Baud rate (Gbaud)	25.0
Symbol number (symbol)	1024
Shift frequency (GHz)	0.0 ~ 50.0
CSPR (dB)	-4.0 ~ 10.0
Roll-off factor	0.05, 0.50, 0.95
Sampling rate (GHz)	100.0
Quantization bit (bit)	2 ~ 8
Wavelength (nm)	1550.0
Total optical power (mW)	1.0
Distance (km)	0, 20
Dispersion coefficient (ps^2/km)	-20.0
Nonlinear index coefficient (1/W/km)	1.27
Loss coefficient (dB/km)	0.2

4. Results

4.1 The Relation between the ADC Sampling Frequency (Bandwidth) and the Shift Frequency

First, we investigated the spectral changes caused during the three nonlinear operations when using the KK reception, square-law detection, logarithm, and square-root calculations, respectively. Figure 5(a) shows the spectrum after direct detection when the shift frequency is 25 GHz. 5(b) and 5(c) depict the spectra after logarithm and square-root calculations of the PD output, respectively. SSBI generated during the square-law detection can be noticed in the direct current (DC) ~12.5 GHz region in Fig. 5(a). Generated harmonic components also can be noticed in the higher frequency region of the intermediate frequency-centered signal

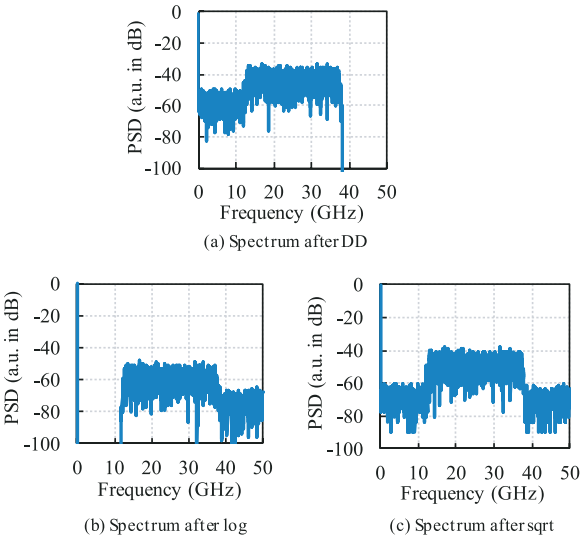

Fig. 5 Spectra after (a) DD, (b) log, (c) sqrt (f_s = 25 GHz).

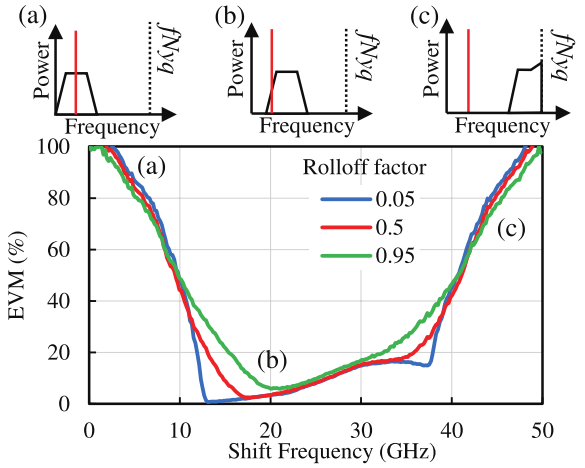

Fig. 6 Relationship between shift frequency and EVM (Roll-off factor 0.05, 0.5, 0.95). Inset; distribution of modulated signal spectrum and the optical tone in regard to Nyquist frequency of ADC.

spectrum of Fig. 5(b), and in the higher frequency regions of Fig. 5(c). It is apparent that the harmonic components are generated during the non-linear operations of the KK algorithm, and the spectrum is spread.

Next, we studied how the signal and the tone's distribution (in the frequency domain) affect KK reception in ADC bandwidth-limited system. Even though the optical tone is added at the transmitter in our system, that can also be done at the receiver. Considering these two scenarios, we measured EVM of the detected signal varying the relative position of the optical tone and the modulated signal spectrum. Figure 6 shows the relationship between the shift frequency and EVM of the detected signal when the ADC sampling frequency is 100 GHz. Here, the roll-off factor α of the RRC filter is selected as to be 0.05, 0.50, and 0.95.

Variations of EVM in regard to the shift frequency show roll-off factor dependence. When the shift frequency is

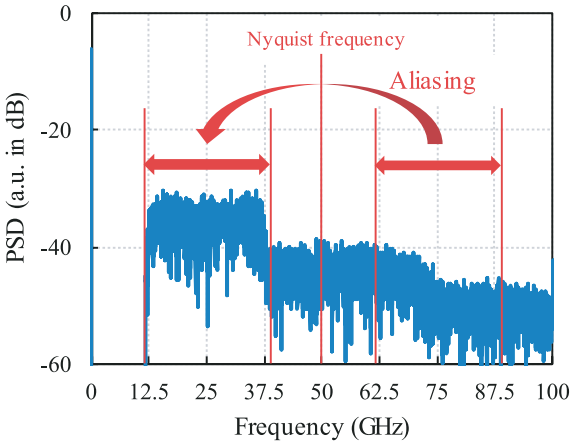

Fig. 7 Aliasing spectrum.

increased from 0 GHz, EVM decreases rapidly. This rapid decrease of EVM is because the increased shift frequency approaches the reception to a minimum-phase condition satisfying process. When the shift frequency is equal to half of the signal band (Baud rate * (1 + α)) corresponding to each roll-off factor, the requirement of the minimum phase condition of KK reception is fulfilled. For the roll-off factor of 0.05, the minimum EVM is achieved at the shift frequency of 13.12 GHz, where the tone lies at the edge of the modulated signal (modulated signal bandwidth = 26.25 GHz).

However, for increased roll-off factors of 0.50 and 0.95, the minimum EVMs are observed at shift frequencies of 17.60 GHz (edge frequency = 18.75 GHz) and 21.09 GHz (edge frequency = 24.37 GHz), respectively. This suggests that the shift frequency which results in the minimum EVM depends not only on the modulated signal bandwidth but also on some other DSP parameters of the system. To further investigate this observation, we investigated aliasing noise in the signal spectrum after processing through the KK algorithm.

Figure 7 shows the aliasing spectrum after performing sqrt and log operations of the KK algorithm when the shift frequency is 25 GHz. Harmonic components exceeding the Nyquist frequency become aliasing and affect the modulated signal spectrum. We calculated the in-band aliasing power (aliasing that overlaps the modulated signal) of log and sqrt calculations. Figure 8(a) and 8(b) show the variations of aliasing power of log and square-root calculations, respectively, with the shift frequency. With increasing shift frequency, in-band aliasing power increases in both cases, suggesting ADC bandwidths' relation to the optimum shift frequency (which results in the minimum EVM). An increase in the roll-off factor results in larger aliasing noise power due to the increased signal bandwidth.

From the above results, the reason for ADC bandwidth dependence of the optimum shift frequency can be explained as follows: in a minimum phase condition fulfilled scenario, EVM increases due to aliasing noise resulted from the broadened spectrum. In-band aliasing noise power increases with increasing roll-off factor (see Fig. 8(a) and (b)).

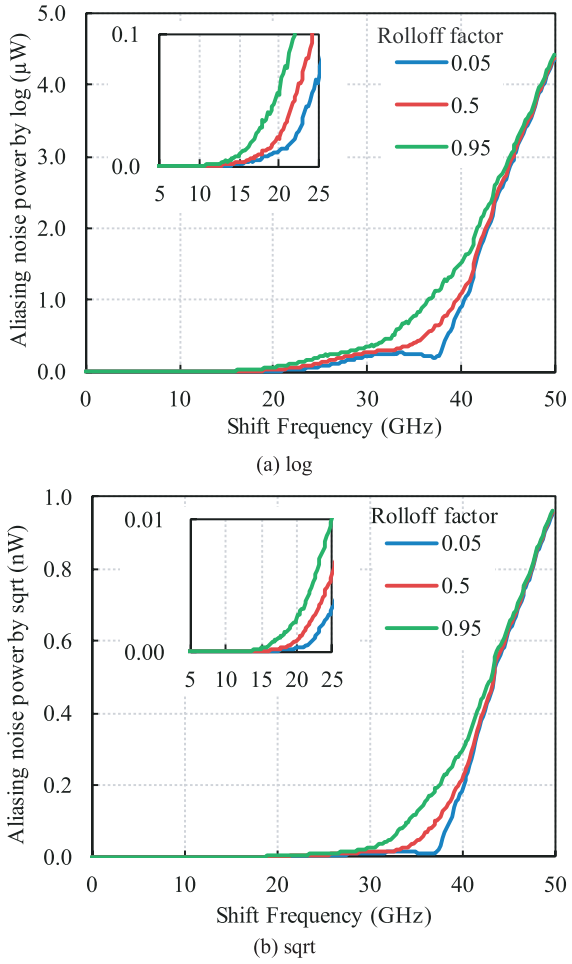

Fig. 8 Aliasing noise power of (a) log, (b) sqrt. Inset; Close-up of shift frequency range 5~25 GHz.

In such environments, the optimum shift frequency exists in in-band where the effect of aliasing noise can be minimized. Here, the penalty caused by the aliasing noise is higher than that caused by placing the optical tone in-band.

In Fig. 6, the EVM gradually increases in the range of 20~30 GHz shift frequencies. This gradual increase of EVM is due to in-band aliasing noise caused by log and sqrt operations.

When the modulated signal exceeds the Nyquist frequency (50 GHz) of the ADC, the EVM rapidly increases. The rapid increase of EVM at about 37 to 50 GHz is caused by the aliasing noise (aliasing of the signal itself) as the modulated signal spectrum exceeds the Nyquist frequency of the ADC as a result of increased shift frequency (see the inset of Fig. 6(c)).

Comparing the aliasing power of logarithm with that of square-root, one can see that the aliasing power of logarithm is larger and it is the dominant cause of EVM increase with increased shift frequency.

4.2 Number of Quantization Bit

The relation between the number of quantization bit and the required CSPR is studied for back-to-back detection. Fig. 9 shows the signal after direct detection when the CSPR of the optical SSB signal is 0, 6, and 10 dB. It can be noticed in the waveforms that the dynamic range of the waveform

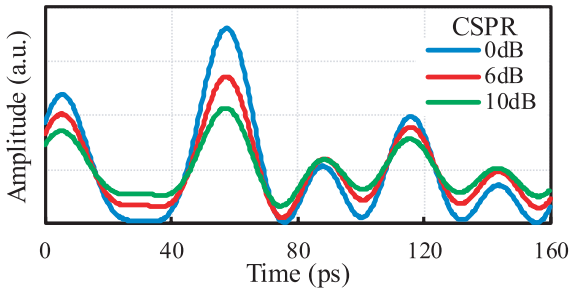

Fig. 9 QPSK waveform after DD.

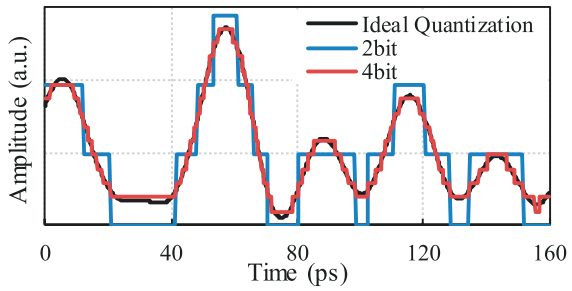

Fig. 10 QPSK waveform after quantization (2, 4 bits) when CSPR = 6 dB.

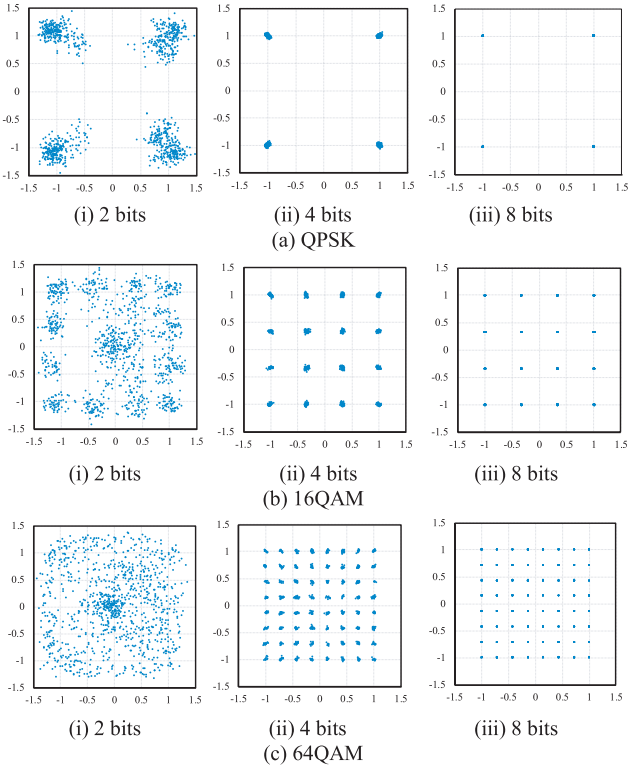

Fig. 11 Back-to-back constellations (CSPR = 10 dB).

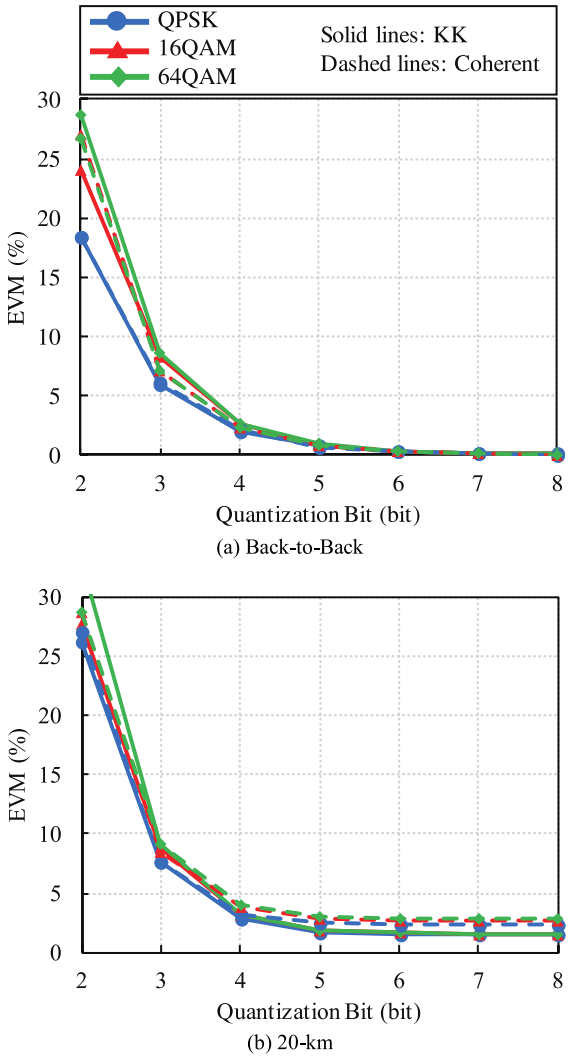

Fig. 12 Relationship between quantization bit and EVM.

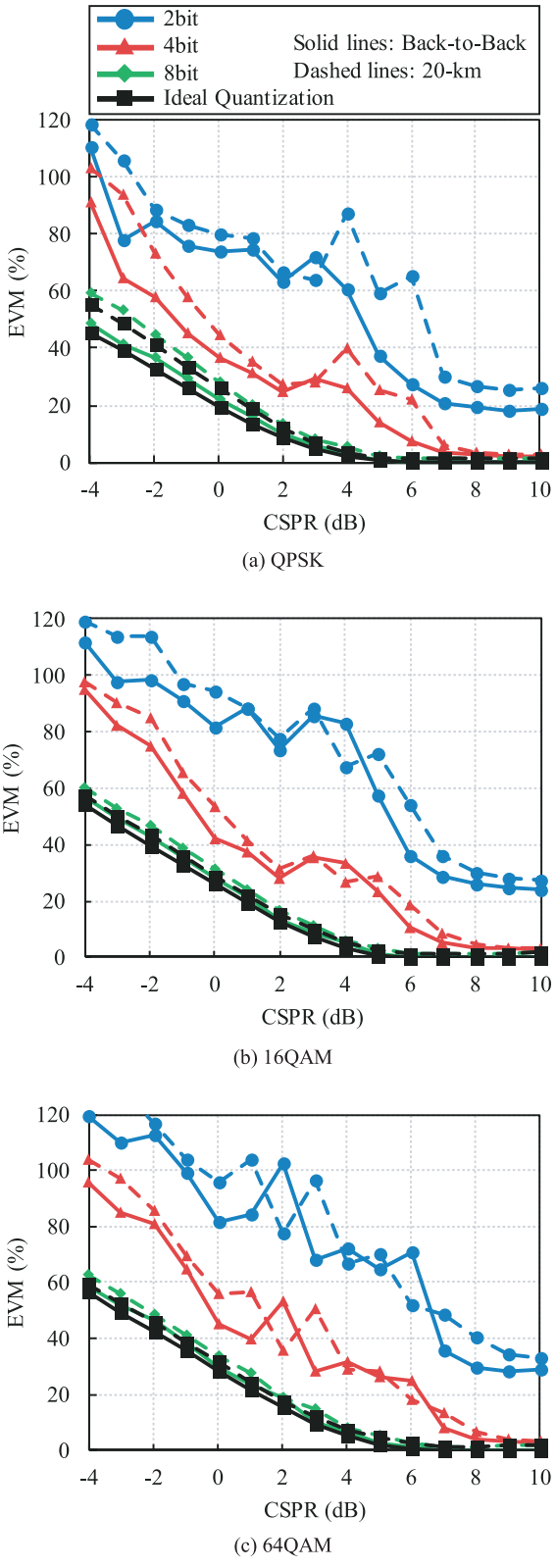

Fig. 13 Relationship between CSPR and EVM.

is reduced with increasing CSPR. For CSPRs greater than 6 dB, the minimum phase condition is satisfied.

Figure 10 presents the waveforms quantized with the quantization bit number of 2 and 4 bits after direct detection of the signal with CSPR of 6 dB. Here, the range of signal amplitude-changes is rescaled during the quantization to match with the fullscale of the ADC. The DC offset is removed before ADC and added back to the AD converted PD output (discrete amplitude).

Varying the number of quantization bit as 2, 4 and 8, the effect of the number of quantization bit on the detected signal constellation is studied for three modulation formats of QPSK, 16-QAM, and 64-QAM. Observed constellations are presented for comparison in Fig. 11 when the CSPR is 10 dB.

One can notice degraded constellations for 2-bit quantization. These constellation distortions are due to limited ADC resolution as we recreated the square-law detected waveform in its original amplitude range. Increasing the number of quantization bit results reduction of constellation distortions.

Measured EVMs of Fig. 11 are presented in Fig. 12(a). Fig. 12(b) depict EVMs after 20-km transmission. For com-

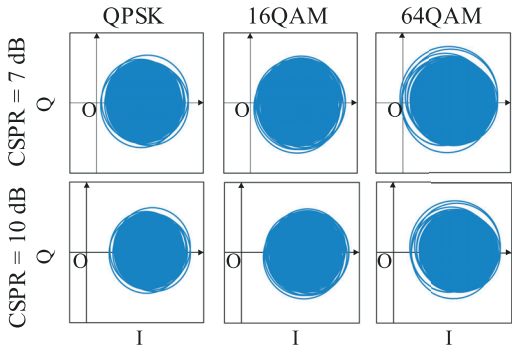

Fig. 14 Optical field trajectories after 20-km transmission.

parison, EVMs of ideal coherent reception is also presented in Fig. 12.

Similar variations of EVM in terms of the number of quantization bits was noticed for both KK and coherent receptions in both back-to-back and 20-km transmitted signals. However, for the coherent reception, it is noteworthy that shown number of quantization bit is only for one dimension (real or imaginary).

We evaluated receiver performance in terms of the number of quantization bits for a back-to-back and 20-km transmitted signal detection, varying CSPR. EVM is plotted against CSPR and compared in Fig. 13 for three different modulation formats QPSK (Fig. 13(a)), 16QAM (Fig. 13(b)) and 64QAM (Fig. 13(c)). Solid lines show back-to-back results and 20-km transmission results are shown in dashed-lines. For back-to-back detection of all three modulation formats, increasing CSPR reduces EVM. For ideal quantization, EVM is 0% when CSPR is greater than 6 dB that satisfies the minimum phase condition. With 2 and 4-bit quantization, EVM is greatly reduced for CSPRs greater than 6 dB for QPSK and 16QAM, and 7 dB for 64QAM.

EVM with 8 bits quantization approximately coincides with the ideal case of quantization for all three modulation formats. When the CSPR is further increased, the EVM gradually decreases and saturates for CSPRs greater than 8 to 9 dB.

Transmission penalties after 20-km transmission were insignificant. To study changes to the minimum phase condition (MPC), we measured optical field trajectories after 20-km transmission. Optical field trajectories of CSPR = 7 dB and 10 dB are presented in Fig. 14 for comparison. For CSPR of 7 dB, we noticed violated MPC in 64QAM transmission while the other two modulation formats remain fulfilling MPC. This explains the slight transmission penalty noticed for 64 QAM. When CSPR = 10 dB, for all the three modulation formats, MPC was satisfied after transmission.

5. Conclusion

We numerically studied the impact of ADC sampling frequency and the number of quantization bit in the direct-detection optical communication system using KK relation. It was found that signal distortions caused by the aliasing noise depends on ADC bandwidth and the shift frequency. Even though there is no need for having a frequency gap between the optical tone and the modulated signal spectrum if the tone is added at the transmitter, adding the tone at the receiver may result in a frequency gap. Those frequency gaps may result in severe signal distortions in ADC bandwidth-limited systems. Sharp anti-aliasing filters will be required in such scenarios to mitigate aliasing-based signal distortions.

The aliasing power caused by the log operation is found to be the dominant factor of signal distortions in the ADC bandwidth limited system. Filtering out of aliasing noise caused by log operation may increase reception performance in such a scenario.

In a system where CSPR is large enough to fulfill the requirement of minimum phase condition, for QPSK, 16-QAM, and 64-QAM modulation formats, we found the minimum EVMs when the number quantization bits is greater than 5.

References

[1] Cisco Systems G.K., "Cisco Global Cloud Index: Forecast and Methodology, 2016-2021 White Paper," https://www.cisco.com/c/en/us/solutions/collateral/service-provider/global-cloud-index-gci/white-paper-c11-738085.html
[2] M. Morsy-Osman and D.V. Plant, "A comparative study of technology options for next generation intra- and inter-datacenter interconnects," Proc. 2018 Opt. Fiber Commun. Conf. and Expo., no.W4E.1, San Diego, CA, USA, March 2018.
[3] N. Kikuchi, "Multilevel signaling technology for increasing transmission capacity in high-speed short-distance optical fiber communication," IEICE Trans. Electron., vol.E102-C, no.4, pp.316–323, April 2019.
[4] N. Kikuchi, "84-, 100-, and 107-GBd PAM-4 intensity-modulation direct-detection transceiver for datacenter interconnects," J. Lightw. Technol., vol.35, no.6, pp.1253–1259, March 2017.
[5] M. Sieben, J. Conradi, and D.E. Dodds, "Optical single sideband transmission at 10 Gb/s using only electrical dispersion compensation," J. Lightw. Technol., vol.17, no.10, pp.1742–1749, Oct. 1999.
[6] N. Kikuchi, R. Hirai, and T. Fukui, "Quasi single-sideband (SSB) IM/DD Nyquist PAM signaling for high-spectral efficiency DWDM transmission," Proc. Opt. Fiber Commun. Conf., no.Th2A.41, Anaheim, California, United States, March 2016.
[7] B.J.C. Schmidt, A.J. Lowery, and J. Armstrong, "Experimental demonstrations of electronic dispersion compensation for long-haul transmission using direct-detection optical OFDM," J. Lightw. Technol., vol.26, no.1, pp.196–203, Jan. 2008.
[8] M. Schuster, S. Randel, C.A. Bunge, and S.C.J. Lee, "Spectrally efficient compatible single-sideband modulation for OFDM transmission with direct detection," IEEE Photon. Technol. Lett., vol.20, no.9, pp.670–672, May 2008.
[9] M.S. Erkilinc, Z. Li, S. Pachnicke, H. Griesser, B.C. Thomsen, P. Bayvel, and R.I. Killey, "Spectrally-efficient WDM Nyquist-pulse-shaped 16-QAM subcarrier modulation transmission with direct detection," J. Lightw. Technol., vol.33, no.15, pp.3147–3155, Aug. 2015.
[10] W. Peng, X. Wu, K. Feng, V.R. Arbab, B. Shamee, J. Yang, L.C. Christen, A.E. Willner, and S. Chi, "Spectrally efficient direct-detected OFDM transmission employing an iterative estimation and cancellation technique," Opt. Express, vol.17, no.11, pp.9099–9111, May 2009.
[11] Z. Li, M.S. Erkilinc, R. Maher, L. Galdino, K. Shi, B.C. Thom-

sen, P. Bayvel, and R.I. Killey, "Two-stage linearization filter for direct-detection subcarrier modulation," IEEE Photon. Technol. Lett., vol.28, no.24, pp.2838–2841, Dec. 2016.

[12] S. Randel, D. Pilori, S. Chandrasekhar, G. Raybon, and P. Winzer, "100-Gb/s discrete-multitone transmission over 80-km SSMF using single-sideband modulation with novel interference-cancellation scheme," Proc. 2015 European Conf. on Opt. Commun., no.0697, Valencia, Spain, Oct. 2015.

[13] C. Ju, N. Liu, X. Chen, and Z. Zhang, "SSBI mitigation in A-RF-tone-based VSSB-OFDM system with a frequency-domain volterra series equalizer," J. Lightw. Technol., vol.33, no 23, pp.4997–5006, Dec. 2015.

[14] Z. Li, M.S. Erikilinc, K. Shi, E. Sillekens, L. Galdino, T. Xu, B.C. Thomsen, P. Bayvel, and R.I. Killey, "Digital linearization of direct-detection transceivers for spectrally efficient 100 Gb/s/λ WDM metro networking," J. Lightw. Technol., vol.36, no.1, pp.27–36, Jan. 2018.

[15] A. Mecozzi, C. Antonelli, and M. Shtaif, "Kramers-Kronig coherent receiver," Optica, vol.3, no.11, pp.1218–1227, Nov. 2016.

[16] Z. Li, M.S. Erkilinc, K. Shi, E. Sillekens, L. Galdino, B.C. Thomsen, P. Bayvel, and R.I. Killey, "SSBI mitigation and Kramers-Kronig scheme in single-sideband direct-detection transmission with receiver-based electronic dispersion compensation," J. Lightw. Technol., vol.35, no.10, pp.1887–1893, May 2017.

[17] Z. Li, M.S. Erkilinc, K. Shi, E. Sillekens, L. Galdino, B.C. Thomsen, P. Bayvel, and R.I. Killey, "Joint optimization of resampling rate and carrier-to-signal power ratio in direct-detection Kramers-Kronig receivers," Proc. 2017 European Conf. on Opt. Commun., no.W.2.D.3, Gothenburg, Sweden, April 2018.

[18] T. Bo and H. Kim, "Kramers-Kronig receiver operable without digital upsampling," Opt. Express, vol.26, no.11, pp.13810–13818, May 2018.

[19] A.J. Lowery, T. Wang, and B. Corcoran, "Clipping-enhanced Kramers-Kronig receivers," Proc. Opt. Fiber Commun. Conf., no.M1H.2, San Diego, California, United States, March 2019.

[20] C. Füllner, M.M.H. Adib, S. Wolf, J.N. Kemal, W. Freude, C. Koos, and S. Randel, "Complexity analysis of the Kramers-Kronig receiver," J. Lightw. Technol., vol.37, no.17, pp.4295–4307, Sept. 2019.

[21] T. Fujita, K. Toba, K.I.A. Sampath, and J. Maeda, "Impact of sampling and quantization on direct-detection lightwave systems using Kramers-Kronig relation," Proc. OptoElec. Commun. Conf., no.TuP4-B8, Fukuoka, Japan, July 2019.

[22] A. Mecozzi, "A necessary and sufficient condition for minimum phase and implications for phase retrieval," arXiv:1606.04861, Oct. 2014.

[23] S.T. Le, K. Schuh, M. Chagnon, F. Buchali, R. Dischler, V. Aref, H. Buelow, and K.M. Engenhardt, "1.72-Tb/s virtual-carrier-assisted direct-detection transmission over 200 km," J. Lightw. Technol., vol.36, no.6, pp.1347–1353, March 2018.

Takaha Fujita was born in Fukuoka, Japan, on Sept. 29, 1996. He received B.S. degrees in electrical engineering from Tokyo University of Science, Chiba, Japan, in 2019. Since 2019, he has joined the graduate school. His research interest is in digital signal processing for optical communications.

Kentaro Toba was born in Tokyo, Japan, on Nov. 12, 1996. He received B.S. degrees in electrical engineering from Tokyo University of Science, Chiba, Japan, in 2019. Since 2019, he has joined the graduate school. His research interest is in digital signal processing for optical communications.

Kariyawasam Indipalage Amila Sampath was born in Elpitiya, Sri Lanka in 1985. He received the B.E., M.E. and Ph.D. degrees from Yamagata University, Yonezawa, Japan in 2012, 2014 and 2017 respectively. Since 2017, he has been with the Department of Electrical Engineering, Faculty of Science and Technology, Tokyo University of Science, Chiba, Japan as an Assistant Professor. His current research interest is focused on spectrally efficient optical transmission systems. Dr. Sampath was the recipient of the Best student paper award of OECC2015 and the Best paper award (2nd place) of ICIIS2017. He is a member of the IEEE, the Optical Society of America, and the Institute of Electronics, Information, and Communication Engineers.

Joji Maeda was born in Tokyo, Japan, on Feb. 21, 1965. He received B.S., M.S. and Ph.D. degrees in electronic engineering from the University of Tokyo, Tokyo, Japan, in 1988, 1990 and 1996, respectively. Since 1993, he has joined the Department of Electrical Engineering, Faculty of Science and Technology, Tokyo University of Science, Chiba, Japan, where he works as a full professor. His current interests involve optical fiber transmission including analog transmission of microwave/millimeter waves, quantum noise in photonic systems, and communication systems in cable television networks. Dr. Maeda is a member of the IEEE (Photonics Society and Communications Society), the Optical Society of America, the Institute of Electronics, Information, and Communication Engineers and the Institute of Image Information and Television Engineers.